

Photodoping and in-gap interface states across the metal-insulator transition in $\text{LaAlO}_3/\text{SrTiO}_3$ heterostructures

Z. Ristic,^{1,2} R. Di Capua,^{1,3} F. Chiarella,¹ G. M. De Luca,¹ I. Maggio-Aprile,² M. Radovic,⁴ and M. Salluzzo^{1,*}

¹*CNR-SPIN, Complesso MonteSantangelo via Cinthia, I-80126 Napoli, Italy*

²*Département de Physique de la Matière Condensée, University of Geneva, 24 Quai Ernest-Ansermet, CH-1211 Geneva 4, Switzerland*

³*Dipartimento Scienze per la Salute, Università del Molise, Via De Sanctis, I-86100 Campobasso, Italy*

⁴*LSNS - EPFL, PH A2 354 (Batiment PH) Station 3 CH-1015 Lausanne, Switzerland*

(Received 22 August 2011; revised manuscript received 11 July 2012; published 23 July 2012)

By using scanning tunneling microscopy/spectroscopy we show that the interface between LaAlO_3 and SrTiO_3 band insulators is characterized by in-gap interface states. These features were observed in insulating as well as conducting $\text{LaAlO}_3/\text{SrTiO}_3$ bilayers. The data show how the interface density of states evolves across the insulating to metal transition, demonstrating that nanoscale electronic inhomogeneities in the system are induced by spatially localized electrons.

DOI: [10.1103/PhysRevB.86.045127](https://doi.org/10.1103/PhysRevB.86.045127)

PACS number(s): 73.20.At, 73.25.+i, 73.43.Jn

I. INTRODUCTION

Interfaces between transition-metal oxides exhibit unique physical phenomena that sensitively depend on the mutual arrangement of single atomic planes, as demonstrated in $\text{LaAlO}_3/\text{SrTiO}_3$ (LAO/STO),^{1–5} $\text{LaTiO}_3/\text{SrTiO}_3$,⁶ and $\text{LaVO}_3/\text{SrTiO}_3$ (Ref. 7) heterostructures. These systems show quasi-two-dimensional metallic behaviors at their interfaces even if their constituents are insulating. For the LAO/STO heterostructures, the conductivity is established at a critical LAO thickness of four unit cells (uc) (Ref. 5) and the metallic system thereby realized behaves as a two-dimensional (2D) electron liquid (2DEL).^{8,9} In addition to the classical structural instability, LAO/STO heterostructures are affected by an electrostatic, polar instability. This instability is believed to drive an electronic reconstruction which consists in a transfer of electrons from the LAO layer to titanium $3d$ states of STO at the interface. However, while some of the predictions based on pure electronic reconstruction models have been confirmed,⁸ theory does not fully describe all the experimental results. For example, the density of mobile electrons forming the 2DEL is one order of magnitude lower than the value expected,^{4,5} and there are increasing evidences that the layers close to the interface are characterized by some amount of chemical disorder.^{10,11}

The ground state is also debated. In particular, magnetic² and 2D-superconducting orders⁴ were found at low temperatures, while recent reports pointed to a possible unconventional coexistence of the two phenomena.^{12–15}

Here we show how the local electronic properties of LAO/STO heterostructures evolve across the insulator-metal transition. Scanning tunneling microscopy/spectroscopy (STM/STS) at room temperature was employed to study bilayers composed by 2uc and 4uc LAO films deposited on TiO_2 terminated (100) SrTiO_3 single crystals. In order to investigate 2uc LAO/STO, which are insulating, we used irradiation by visible light as a nondestructive method to induce carriers in the system. STS showed that visible light promotes electrons into in-gap interface states (IGISs) of 2uc LAO/STO. In-gap states are observed also in conducting 4uc LAO/STO, independently on the presence of visible light, but they are arranged in nanometer-size patches. The data

show that a fraction of the electrons necessary to solve the polar instability are spatially localized in these interface states.

STM/STS was performed at room temperature in ultrahigh vacuum (UHV) using a VT-AFM Omicron scanning probe microscope. An incandescence lamp with a tungsten filament, placed outside the UHV chamber, was used to illuminate the sample surface. To eliminate any ultraviolet component, a lead glass was placed between the source and the UHV quartz window in front of the sample holder.

The LAO/STO bilayers were prepared by pulsed laser deposition in 8×10^{-5} mbar of O_2 pressure at 780°C and annealed after the deposition in an oxygen atmosphere.⁵ Contacts were directly deposited onto the interface. Samples with a LAO thickness below 4uc, kept in dark, are insulating. In particular, a 2uc LAO/STO did not show a measurable in-plane conductivity. However, tunneling into the interface was achieved by illuminating the sample in UHV and by using tunneling resistances above $1\text{ T}\Omega$ (tunneling current of 1 pA at 1 V). The data were recorded in the $-1.5\div 1.5\text{-V}$ bias voltage range, where no states from the LAO surface are available in the tunneling process. Indeed, the conduction-band minimum of LAO is 2.2 eV above the STO one, while the valence band of LAO is $2.3\text{--}2.5\text{ eV}$ below the Fermi level. Therefore the spectra are representative of the interface electronic properties.^{9,16}

Figures 1(a) and 1(b) show contact AFM images acquired in UHV on a 2uc and 4uc LAO/STO, respectively. The AFM morphology of the LAO surfaces is characterized by regularly spaced terraces and step edges, reminiscent of the morphology of the STO substrate. However, each terrace shows atomic-layer hills-valleys modulations on several nanometers lateral scales, demonstrating that the LAO surface planes are incomplete.¹⁶ Figure 1(c) shows an STM image acquired at 1 V and 0.25 pA on the same 2uc with light on. The tunneling conditions cannot be stabilized by turning off the visible light, showing that tunneling is possible only because of photodoping effects. An STM image acquired in similar conditions on a metallic 4uc LAO/STO is shown in Fig. 1(d). Since the bias voltage used is well below the conduction-band minimum of LAO, Figs. 1(c) and 1(d) represent STM topographies of the interfaces.⁹ The interfaces

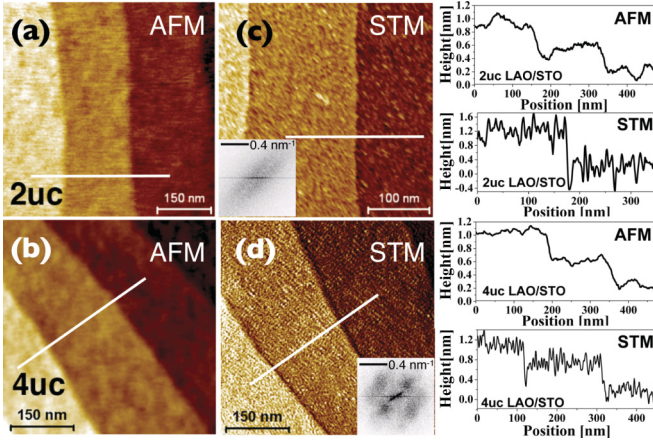


FIG. 1. (Color online) Contact AFM topography of the LAO surface in UHV of (a) 2uc and (b) 4uc LAO/STO interface (z scale, max to min 0–1.4 nm and 0–1.5 nm, respectively). (c) STM topography on the same 2uc ($V_{\text{bias}} = +1.0$ V, $I_t = 0.25$ pA, light on) and (d) 4uc samples ($V_{\text{bias}} = +1.0$ V, $I_t = 0.5$ pA, light off). The min to max z scale is 0–2.0 nm in (c) and 0–2.2 nm in (d). Height profiles taken along the lines are also shown on the right. The insets of (c) and (d) are the 2D Fourier power spectra of the corresponding topographic images.

are also characterized by terraces and step edges, but they do not exhibit the same hill-valley layer modulation characteristic of the surfaces and shown by contact AFM. Moreover, in both 2uc and 4uc LAO/STO the apparent interface roughness is higher than the roughness of the topmost LAO surfaces.

A very intriguing feature of metallic LAO/STO interface is the presence of a quasiperiodic nanoscale modulation of the density of states, also visible in the STM topography,⁹ as shown in Fig. 1(d). On the other hand, no superstructure is observed in the case of 2uc LAO/STO interface [Fig. 1(c) and inset]. This is an important difference between insulating and conducting LAO/STO. In fact this result indicates that while the interfaces are not atomically sharp in both cases,^{10,11,16} only 4uc LAO/STO shows signatures of an electronic reconstruction.

In order to identify the distinctive electronic properties of 2uc and 4uc LAO/STO samples, we recorded point-by-point spectroscopy maps, i.e., spatially resolved I vs V and dI/dV vs V spectra. Since the tunneling current changes exponentially as a function of the LAO thickness, we show here both dI/dV vs V and $(dI/dV)/(I/V)$ (normalized conductance) data. Note that the normalized conductance is in part able to account for the thickness and energy dependence of the tunnel barrier. Finally, spectroscopy gap maps were also extracted from the dI/dV spectra by using a threshold criteria, e.g., a threshold of 2% of the tunneling conductance that corresponds to 0.01 pA/V for a junction with conductance of 0.5 pA/V.

The dI/dV tunneling spectra of 2uc LAO/STO under light show a prominent asymmetry, in particular a gap around the Fermi level and a maximum around -1.0 ± 0.1 V (occupied states) [Figs. 2(a)–2(c)]. On the unoccupied side the tunnel conductivity shows also a shoulder around $+1.0$ V. These results are confirmed by the analysis of the normalized $(dI/dV)/(I/V)$ spectra that exhibit two peaks around -1.0 V and $+1.0$ V [Fig. 2(b)]. These features are reproduced in any

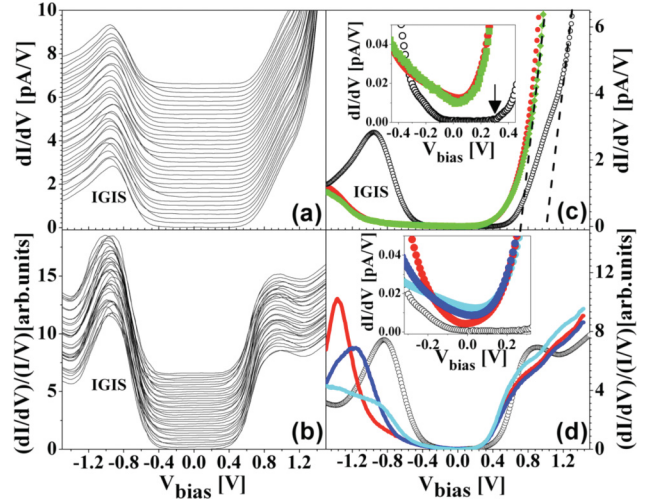


FIG. 2. (Color online) (a) Sequences of dI/dV and (b) normalized $(dI/dV)/(I/V)$ spectra of a 2uc LAO/STO acquired with light on along a line on a single terrace; the spectra are separated by 1 nm distance one from the other. (c) Comparison between the average dI/dV of a 2uc (black open circles, light on) and 4uc LAO/STO (green closed squares light on, red closed circles light off). Dashed lines show the positions of the leading edges of the conduction bands in the two samples. The inset of Fig. 2(c) shows the same dI/dV spectra around the Fermi level. The arrow indicates the point at which the dI/dV of 2uc LAO/STO is above a zero value. (d) $(dI/dV)/(I/V)$ average spectra of a 2uc LAO/STO (open circles) compared to the data acquired on 4uc LAO/STO (continuous red, cyan, and blue lines). The three spectra shown for 4uc LAO/STO describe the spatial variation of its electronic properties. The inset of Fig. 2(d) shows the corresponding dI/dV curves around the Fermi level.

location, as shown by the sequence of spectra taken along a single line on a terrace [Figs. 2(a) and 2(b)]. The $+1.0$ V peak could be identified as a feature of the STO conduction band, due to unoccupied titanium 3d states. The peak at -1.0 V, on the other hand, is not related to the STO valence band, that is expected to be 2.5 eV below the Fermi level. Thus this feature is indicative of a characteristic in-gap interface state (IGIS). The IGIS is present everywhere, however its intensity and its energy position change as a function of the location on the interface, as shown by the $(dI/dV)/(I/V)$ map at -1.0 V of Fig. 3(b). The gap map of Fig. 3(c) confirms the inhomogeneous electronic properties and the nonmetallic character of 2uc LAO/STO interfaces exposed to visible light.

The dI/dV spectra of a 4uc LAO/STO samples shows characteristics that are quite different from the one of 2uc LAO/STO, which are independent on the irradiation by visible light and remain unchanged by performing measurements in dark conditions [Fig. 2(c)]. First of all, the tunneling conductance of a metallic interface is characterized by a small but finite value at the Fermi level [inset of Fig. 2(c)]. The conduction-band minimum is below the Fermi level in the case of 4uc LAO/STO samples, while it is 0.3 eV above the Fermi level in 2uc LAO/STO. Additionally, the leading edges of the conduction bands are at $+0.6$ V and $+1.0$ V in 4uc and 2uc LAO/STO, respectively. Thus, by analyzing the spectra obtained on LAO/STO bilayers with LAO thicknesses

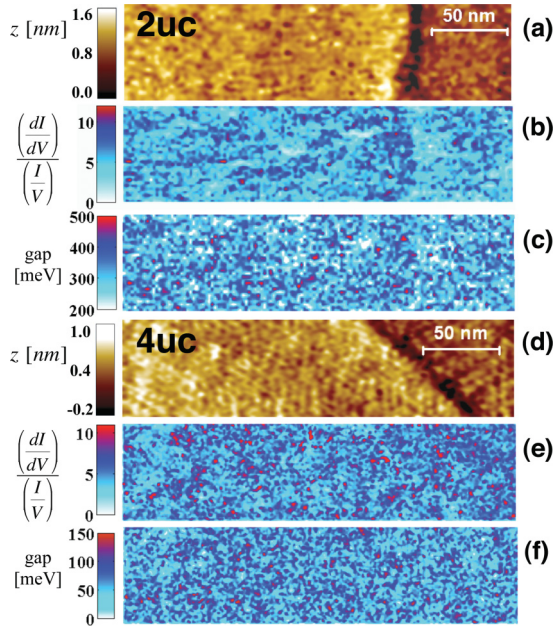


FIG. 3. (Color online) (a) Topography (+1.2 V, 0.75 pA), (b) $(dI/dV)/(I/V)$ map measured at -1.0 V and (c) gap map (see text) on a 2uc LAO/STO. (d) Topography (+1.0 V, 0.5 pA), (e) $(dI/dV)/(I/V)$ map measured at -1.3 V and (f) gap map (see text) on a 4uc LAO/STO (Ref. 16).

of 2uc and 4uc, we conclude that the conduction band shifts towards the Fermi level by 0.3–0.4 eV across the insulating to metal transition. This result is in agreement with recent theoretical calculations predicting a band bending of 0.37 eV in the case of full compensation of the polar discontinuity.¹⁷ Similar, but somewhat reduced, shifts of core-level states shown by photoemission spectroscopy in LAO/STO heterostructures¹⁸ were also attributed to band bending effects.

The differences between the electronic properties of 4uc and 2uc LAO/STO samples are even better revealed by an analysis of the $(dI/dV)/(I/V)$ data. In Fig. 3(d) we show the main typologies of normalized conductance spectra of 4uc LAO/STO, statistically determined from a whole set of spectroscopy maps obtained on one of the samples investigated. The first kind of spectra, observed in sparse regions of the interface, displays a well-defined peak at -1.3 V [red line in Fig. 2(d), 10–15% of coverage]. This feature indicates the presence of interface states with energies well below the Fermi level also in conducting samples. The $(dI/dV)/(I/V)$ map acquired at -1.3 V, shown in Fig. 3(e), provides a direct visualization of the spatial distribution of this feature, where it shows up as a few nm's wide bright (red) patches. The remaining regions are characterized by other two typologies of spectra, which differ for both occupied and unoccupied states, i.e., spectra still showing a broader peak at lower bias of -1.2 V [blue line in Fig. 2(d), blue pixels in Fig. 3(e), 35–40% of coverage] and spectra that do not show any peak in the occupied density of states [cyan line in Fig. 2(d), blue pixels in Fig. 3(e)]. We also find that areas showing a peak in the $(dI/dV)/(I/V)$ are also characterized by the opening of a small gap (50–150 meV) [Fig. 3(f)], i.e., spectral weight is moved from states close to the Fermi level to states well below

the Fermi level.¹⁶ Finally, we note that the in-gap interface states in 4uc LAO/STO move to higher energies compared to 2uc LAO/STO, in quantitative agreement with the 0.3–0.4-eV shift of the conduction band across the insulating to metal transition [Fig. 2(c)]. Consequently, this result is explained by the presence of a band bending potential at the metallic interface.

II. DISCUSSION

The experimental data show that conducting LAO/STO interfaces are characterized by nanoscale spatial electronic inhomogeneities [see Figs. 2(d), 3(e), and 3(f), and Ref. 16]. In particular, a distinctive characteristic of electronically reconstructed LAO/STO is the presence of a quasiperiodic modulation of the density of states, as discussed in Ref. 9. This feature is absent in insulating 2uc LAO/STO, thus it is a consequence of the realization of a 2DEL at the interface. On the other hand, both insulating and metallic LAO/STO show in-gap interface states. In the case of 2uc samples, these states are partially filled by photodoped electrons and are observed everywhere, while in 4uc LAO/STO in-gap interface states are already occupied, without the need of photodoping effects, and are spatially distributed forming nanometer patches. Interestingly, these patches cover about 50% of the metallic interfaces, if we consider together regions characterized by the intense IGIS [bright (red) pixels in Fig. 3(e)] and regions showing a less intense and broader peak [blue pixels in Fig. 3(e)].

In-gap interface states in LAO/STO heterostructures, and related electronic inhomogeneities, are not predicted by theoretical calculations based on an ideal electronic reconstruction picture.^{17,19} Thus an explanation of their origin is an important step towards a better understanding of the electronic properties of this system. First, we exclude that these inhomogeneities are due to a possible modulation of the electrostatic potential associated to an imperfect termination of the LAO surface (Fig. 1). Indeed, in the case of metallic LAO/STO, spectra showing the IGIS are separated by the others on nanometer scales [Fig. 3(b)], while areas with an imperfect atomic termination of the LAO surface [Fig. 1(b)] have sizes of several nanometers, demonstrating that there is no direct relationship between surface and interface electronic inhomogeneities measured by STS.

Another possible origin of in-gap states is chemical disorder. In particular, in-gap interface states found in the case of *in situ* fractured/cleaved STO²⁰ by photoemission were attributed to oxygen vacancies. This interpretation, in the case of STO surfaces, was supported by atomically resolved STS on $\sqrt{5} \times \sqrt{5} - R26.6^\circ$ reconstructed SrTiO₃ single crystals,²¹ and later on by local-density approximation + on-site repulsion (LDA + U) calculations.²² However, the spatial density of the IGIS is so high that only an unrealistic amount of oxygen vacancies would explain the data in both 2uc and 4uc LAO/STO interfaces. Moreover, this idea contradicts other characterizations, which have set an upper limit to the amount of oxygen vacancies in LAO/STO interfaces annealed in O₂ after the deposition to 3–5%.³ Similar arguments allow us to exclude cation disorder to explain the results, since the ubiquitous observation of an IGIS in 2uc LAO/STO

would require an amount of disorder larger than the one of metallic 4uc LAO/STO, which is also contradicted by the experiments.^{10,16}

Thus the data analysis suggests that in-gap interface states are an intrinsic feature of the LAO/STO system. In 2uc LAO/STO visible light is unable to excite photodoped electrons to the interface conduction band, but it induces spatially localized electrons in the in-gap interface states. In 4uc LAO/STO, on the other hand, our results suggest that a large fraction of electrons, up to 50% if we count all the spectra characterized by an IGIS, are also localized at the interface. This number is similar to the fraction of electrons necessary to solve the polar catastrophe. Consequently, a complete compensation of the electrostatic potential is not only achieved by the formation of a mobile electron gas, but also by transfer of a large fraction of localized electrons. This characteristic is likely related to the general doping mechanism of titanate surfaces. Resonant photoemission²³ showed that even in metallic Nb-doped STO, beside delocalized electrons with mainly Ti 3d character, a non-negligible spectral weight is transferred to incoherent states (localized states) in the gap. These states are due to the hybridization between the transition-metal 3d levels and the oxygen 2p levels. Thus the most plausible explanation of the IGIS is the realization of nominal Ti³⁺ ions that, with their charge screened by the surrounding oxygen cage, act as effective impurity centers creating multiple charge states below the Fermi level.²⁴ An alternative picture, proposed in Ref. 25, is the realization of a 2D polaronic phase due to a strong electron-lattice interaction, inducing spatially localized

unpaired electrons on individual Ti sites. The presence of localized and delocalized electrons is consistent with second harmonic generation,²⁶ resonant inelastic x-ray scattering²⁷ and photoemission spectroscopy^{28,29} experiments. Thus, according to these scenarios, the doping process itself would intrinsically induce occupied in-gap interface states and will originate a spatial modulation of the local density of states. We argue that this kind of intrinsic electronic effects, which are typical of correlated oxides, could drive different ground states²⁵ and possibly exotic magnetic and superconducting orders at low temperatures.¹²⁻¹⁵

III. CONCLUSION

In conclusion, by using scanning tunneling microscopy/spectroscopy we have shown that the interface between LaAlO₃ and SrTiO₃ band insulators is characterized by in-gap interface states in both insulating and metallic cases. The data are explained by assuming that a considerable fraction of the electrons transferred are localized around the nominal Ti³⁺ dopant ions, so that nanoscale modulation of the density of states are induced in the system.

ACKNOWLEDGMENTS

The authors acknowledge C. Richter for growing the excellent LAO/STO films studied. Discussions with J. Mannhart, N. Pavlenko, A. Perroni, A. Filippetti, S. Gariglio, and J.-M. Triscone were very valuable for the interpretation of the experimental results.

*salluzzo@na.infn.it

¹A. Ohtomo and H. Y. Hwang, *Nature (London)* **427**, 423 (2004).

²A. Brinkman *et al.*, *Nat. Mater.* **6**, 493 (2007).

³N. Reyren *et al.*, *Science* **317**, 1196 (2007).

⁴A. D. Caviglia, S. Gariglio, C. Cancellieri, B. Sacepe, A. Fete, N. Reyren, M. Gabay, A. F. Morpurgo, and J. M. Triscone *Phys. Rev. Lett.* **105**, 236802 (2010).

⁵S. Thiel, G. Hammerl, A. Schmehl, C. W. Schneider, and J. Mannhart, *Science* **313**, 1942 (2006).

⁶A. Ohtomo, D. A. Muller, J. L. Grazul, and H. Y. Hwang, *Nature (London)* **419**, 378 (2002).

⁷Y. Hotta, T. Susaki, and H. Y. Hwang, *Phys. Rev. Lett.* **99**, 236805 (2007).

⁸M. Breitschaft *et al.*, *Phys. Rev. B* **81**, 153414 (2010).

⁹Z. Ristic, R. Di Capua, G. M. De Luca, F. Chiarella, G. Ghiringhelli, J. C. Cezar, N. B. Brookes, C. Richter, J. Mannhart, and M. Salluzzo, *Europhys. Lett.* **93**, 17004 (2011).

¹⁰S. A. Pauli, S. J. Leake, B. Delley, M. Bjorck, C. W. Schneider, C. M. Schlepütz, D. Martocchia, S. Paetel, J. Mannhart, and P. R. Willmott, *Phys. Rev. Lett.* **106**, 036101 (2011).

¹¹R. Yamamoto, C. Bell, Y. Hikita, H. Y. Hwang, H. Nakamura, T. Kimura, and Y. Wakabayashi, *Phys. Rev. Lett.* **107**, 036104 (2011).

¹²Ariando *et al.*, *Nat. Commun.* **2**, 188 (2011).

¹³L. Li, C. Richter, J. Mannhart, and R. C. Ashoori, *Nat. Phys.* **7**, 762 (2011).

¹⁴J. A. Bert, B. Kalisky, C. Bell, M. Kim, Y. Hikita, H. Y. Hwang, and K. A. Moler, *Nat. Phys.* **7**, 767 (2011).

¹⁵D. A. Dikin, M. Mehta, C. W. Bark, C. M. Folkman, C. B. Eom, and V. Chandrasekhar, *Phys. Rev. Lett.* **107**, 056802 (2011).

¹⁶See Supplemental Material at <http://link.aps.org/supplemental/10.1103/PhysRevB.86.045127>.

¹⁷Pietro Delugas, A. Filippetti, V. Fiorentini, D. I. Bilc, D. Fontaine, and P. Ghosez, *Phys. Rev. Lett.* **106**, 166807 (2011).

¹⁸K. Yoshimatsu, R. Yasuhara, H. Kumigashira, and M. Oshima, *Phys. Rev. Lett.* **101**, 026802 (2008).

¹⁹Z. S. Popovic, S. Satpathy, and R. M. Martin, *Phys. Rev. Lett.* **101**, 256801 (2008).

²⁰Y. Aiura, I. Hase, H. Bando, Y. Yasue, T. Saitoh, and D. S. Dessau, *Surf. Sci.* **515**, 61 (2002).

²¹H. Tanaka, T. Matsumoto, T. Kawai, and S. Kawai, *Jpn. J. Appl. Phys.* **32**, 1405 (1993).

²²Z. Fang and K. Terakura, *Surf. Sci. Lett.* **470**, L75 (2000).

²³Y. Ishida, R. Eguchi, M. Matsunami, K. Horiba, M. Taguchi, A. Chainani, Y. Senba, H. Ohashi, H. Ohta, and S. Shin, *Phys. Rev. Lett.* **100**, 056401 (2008).

²⁴F. D. M. Haldane and P. W. Anderson, *Phys. Rev. B* **13**, 2553 (1976).

²⁵B. R. K. Nanda and S. Satpathy, *Phys. Rev. B* **83**, 195114 (2011).

²⁶A. Savoia *et al.*, *Phys. Rev. B* **80**, 075110 (2009); A. Rubano *et al.*, *ibid.* **83**, 155405 (2011).

²⁷Ke-Jin Zhou, M. Radovic, J. Schlappa, V. Strocov, R. Frison, J. Mesot, L. Patthey, and T. Schmitt, *Phys. Rev. B* **83**, 201402 (2011).

²⁸G. Drera *et al.*, *Appl. Phys. Lett.* **98**, 052907 (2011).

²⁹M. Takizawa, S. Tsuda, T. Susaki, H. Y. Hwang, and A. Fujimori, *Phys. Rev. B* **84**, 245124 (2011).